

A Compressive Sensing Approach for Connected Vehicle Data Capture and Recovery and its Impact on Travel Time Estimation

Lei Lin, Weizi Li, and Srinivas Peeta

Abstract— Connected vehicles (CVs) can capture and transmit detailed data such as vehicle position and speed through vehicle-to-vehicle and vehicle-to-infrastructure communications. The wealth of CV data brings new opportunities to improve the safety, mobility, and sustainability of transportation systems. However, the potential data explosion is likely to over-burden storage and communication systems. To mitigate this issue, we propose a compressive sensing (CS) approach that allows CVs to capture and compress data in real-time and later recover the original data accurately and efficiently. We evaluate our approach using two comprehensive case studies. In the first study, we apply our approach to re-capture 10 million CV Basic Safety Message (BSM) speed samples from the Safety Pilot Model Deployment program. As a result, our approach can recover the original speed data with the root-mean-squared error as low as 0.05. We have also explored the recovery performances of our approach regarding other BSM variables in detail. In the second study, we have built a freeway traffic simulation model to evaluate the impact of our approach on travel time estimation. Multiple scenarios with various CV market penetration rates, On-board Unit (OBU) capacities, compression ratios, arrival rate patterns, and data capture rates are simulated. The simulation results show that our approach provides more accurate estimation than conventional data collection methods up to 65% relative reduction of travel time estimation error. We also observe that when the compression ratio is low, our approach can still provide accurate estimations, hence reducing the OBU hardware cost. Last, our approach can greatly improve the accuracy of the travel time estimations when CVs are in traffic congestion. This is due to that our approach provides a broader spatial-temporal converge of traffic conditions and can accurately and efficiently recover the original CV data.

Index Terms—Compressive Sensing, Connected Vehicle, Compression Ratio, Discrete Cosine Transform, Signal Recovery, Travel Time Estimation, Traffic Simulation.

I. INTRODUCTION

RECENT advancements in technology and its implication on socio-economic benefits of improved traffic conditions have prompted widespread research and development of connected vehicles (CVs). These machineries promise to

This work is supported by the NEXTRANS Center at Purdue University, and CCAT, the Region 5 University Transportation Center.

L. Lin is with the NEXTRANS Center, Purdue University, West Lafayette, IN 47906 USA (e-mail: lin954@purdue.edu).

improve the safety and mobility of our transportation system by enhancing situational awareness [1], [2] and traffic state estimation [3] through vehicle-to-vehicle (V2V) and vehicle-to-infrastructure (V2I) communications.

As an example of such endeavors, in 2012, the Safety Pilot Model Deployment (SPMD) program was launched in Ann Arbor, Michigan, United States. Nearly 3000 vehicles were equipped with GPS antennas and DSRC (Dedicated Short-Range Communications) devices. Each vehicle broadcasted Basic Safety Messages (BSMs), which include the position, velocity, and yaw rate, to nearby CVs and roadside units at a rate of 10 Hz [4]. These CV data bring opportunities for improving intelligent transportation system applications such as traffic state estimation and traffic signal optimization. However, the high-sampling-rate (i.e., 10 Hz), which can result in 25GB data being captured and uploaded every hour [5], gives rise to the prohibitive cost of storage and communication systems. According to Muckell et al. [6], the annual cost of tracking a fleet of 4000 vehicles ranges from \$1.8 million to \$2.5 million. Due to the rapid vehicle production and increasing market penetration rate (MPR) of CVs, this cost is expected to undergo substantial growth in the near future.

Addressing this challenge, previous studies have mainly taken two approaches. The first is called sample-then-compression, which collects data at a fixed rate in real-time and compresses the data offline. To list few examples, the Douglas-Peucker algorithm is one of the classical sample-then-compression methods proposed in 1973 [7]. Richter et al. (2012) introduced a semantic trajectory compression method, which utilizes reference points in a transportation network to replace raw and redundant GPS trajectory data points [8]. Popa et al. (2015) proposed an extended data model and a transportation network partitioning algorithm to increase the trajectory compression rates without increasing the compression error [9]. The limitation of the first approach is that no optimal solution is provided to adjust the online data sampling rate. Hence redundant information is still captured, transmitted and stored.

W. Li is with Department of Computer Science, University of North Carolina at Chapel Hill, Chapel Hill, NC 27599 USA (e-mail: weizili@cs.unc.edu).

S. Peeta is with School of Civil Engineering, Purdue University, West Lafayette, IN 47906 USA, and also with the NEXTRANS Center, Purdue University, West Lafayette, IN 47906 USA (e-mail: peeta@purdue.edu).

In contrast, the second approach has adopted a dynamic perspective by reducing the amount of data captured online while not compromising system awareness and control requirements of transportation authorities. As an example, the concept of Dynamic Interrogative Data Capture (DIDC) is proposed [10]. The basic idea of DIDC is to identify the lowest data capture and transmission rate while satisfying a certain performance measure request (e.g., system-wide travel time estimation or shockwave location in a specific link). In the situation of multiple requests, a DIDC controller will conduct a heuristic optimization routine to prioritize the most important one. Though effective, the DIDC controller may cause conflicts among received requests. In addition, the prioritization and sorting tasks of the requests are non-trivial. As another example, Płaczek [11] developed a framework that dynamically adjusts the data capture rate based on the uncertainty of control decisions instead of the performance measures. The data are collected only when the uncertainty is higher than a predefined threshold, and the uncertainty of traffic control decisions is quantified through the fuzzy number comparison approach [12]. The main issue of the second approach is that the data collected are limited to specific tasks and time periods, which poses higher requirements for the scalability and stability of data analysis algorithms.

In this work, we propose a compressive-sensing (CS) based approach for CV data capture and recovery. We also evaluate its impact on travel time estimation. CS has become an active research topic in recent years as a novel approach to capture and recover signals [13]–[15]. Differing from the first approach in which huge amount of data are acquired and compressed, CS enables redundancy removal during the sampling process via a lower but more effective sampling rate [16]. Unlike the second approach, CS does not require dynamic adjustment to the data capture rate based on various performance measures [10] or traffic control applications [11]. Instead, it performs a linear transformation to capture the essence of a signal [17], which then can be used to recover the signal for various purposes. The high resemblance of the recovered and original signals allows existing data analysis algorithms to continue function without any modification.

In the transportation domain, CS has only been applied for interpolating missing sensor data from loop detectors or probe vehicles to estimate traffic states. Li et al. (2011) tried to estimate traffic states based on trajectory data of taxis in an urban environment. They applied the CS algorithm for scenarios when the spatial and temporal trajectory data are missing [18]. Zheng and Su (2016) applied a novel algorithm based on the CS theory to recover missing traffic flow data from loop detectors and showed it performs better than the Kalman filter based model [19]. Li et al. (2017) developed a novel framework based on the CS theory to estimate city-wide travel times using sparse GPS traces [20]. Our method differs from these studies by applying the CS theory for online CV data capture and storage rather than offline processing.

The contribution of this paper is twofold. First, we aim to design a CS-based approach for CV data capturing so that less information needs to be stored and transmitted. Our approach is

straightforward and can be easily implemented with the current CV data capture approach. To be specific, a CV still examines data samples at a fixed rate, except our approach determines whether to keep a sample or not. Furthermore, our approach allows one to recover the captured data with high accuracy. We evaluate our approach using 10 million CV data samples from the SPMD program. As a result, we can recover the CV data with the root mean squared error (RMSE) of 0.05 by keeping only 20% of the original data (i.e., reducing the storage and transmission cost by 80%).

Second, we have built a simulation model for a five-mile two-lane freeway segment to evaluate the impact of our approach on travel time estimation. In particular, we compare our approach along with two conventional techniques (i.e., the one using only loop detector data and the one using high-sampling CV data) to the ground truth values. As a result, our approach can generate the most accurate travel time estimations in all simulation scenarios especially the congested ones. Comparing to high-sampling CV data, the largest relative reduction of travel time estimation error using our approach can reach 65%. This study also implies that our approach allows a CV to have a smaller on-board unit (OBU) capacity thus reduces the equipment cost.

The rest of the paper is organized as follows. Next section introduces basic CS theory and the CS approach for CV data capture and recovery. Following that, two case studies are presented: applying the CS approach for the compression and recovery of 10 million BSM speed samples, and evaluating the impact of the CS approach on travel time estimation. Finally, the paper concludes with discussion of experimental findings and future research directions.

II. METHODOLOGY

This section introduces the basic concepts of CS theory and our approach for data capture and recovery.

A. Background

Consider a signal vector $x \in R^N$. It can be represented in terms of a set of orthonormal basis $\{\Psi_i\}_{i=1}^N$, $\Psi_i \in R^N$ as:

$$x = \Psi\alpha, \quad (1)$$

where Ψ is an $N \times N$ matrix called Sparsifying Matrix. The signal x is K -sparse if α , the transformed coefficient vector, has K nonzero entries.

Using the traditional data compression approach (i.e., sample-then-compression), the full signal vector x needs to be acquired first, then the vector α is computed through $\alpha = \Psi^T x$ and only the K largest coefficients are kept [21].

In contrast, CS directly acquires a compressed signal through the following sampling process:

$$y = \Phi x = \Phi \Psi \alpha = \Theta \alpha, \quad (2)$$

where $\Theta = \Phi \Psi$ is an $M \times N$ matrix. $y \in R^M$ is the sampled vector, $M \ll N$. Φ is an $M \times N$ matrix called Sensing Matrix.

M and N determine the compression ratio computed as M/N .

Equation (2) defines an underdetermined linear system. Because the number of equations (i.e., M) is much less than the number of unknown entries (i.e., N) [16]. The K -sparse x can be recovered from y which consists of M measurements by solving the following l_0 -norm minimization problem:

$$\operatorname{argmin}_{\alpha} \|\alpha\|_0, \text{ subject to } \Theta\alpha = y, \quad (3)$$

where the l_0 -norm $\|\alpha\|_0$ indicates the number of non-zero elements in the vector denoting the signal's sparsity. Equation (3) represents an NP-hard problem and has no efficient solutions.

The CS theory mediates this issue by introducing the following definition [22]: Matrix A satisfies the restricted isometry property (RIP) of order K , if there exists a constant $\delta_K \in (0,1)$ such that:

$$(1 - \delta_K)\|v\|_2^2 \leq \|Av\|_2^2 \leq (1 + \delta_K)\|v\|_2^2, \quad (4)$$

for $\forall v$ satisfying $\|v\|_0 \leq K$.

If the matrix Θ satisfies the RIP of order $2K$ which can be represented as Equation (5), an accurate reconstruction of a signal can be obtained by solving the following l_1 -norm optimization problem in Equation (6) [22]:

$$(1 - \delta_{2K})\|v\|_2^2 \leq \|\Theta v\|_2^2 \leq (1 + \delta_{2K})\|v\|_2^2, \quad (5)$$

where $v = \alpha_1 - \alpha_2$ and $\|v\|_0 \leq 2K$.

$$\operatorname{argmin}_{\alpha} \|\alpha\|_1, \text{ subject to } \Theta\alpha = y. \quad (6)$$

The rationale is that the distance between any pair of K -sparse signals α_1 and α_2 will not be stretched or compressed to a large degree during the dimension reduction from $\alpha \in R^N$ to $y \in R^M$ such that the salient information of a K -sparse signal is preserved [21]. Equation (6) can be solved via linear programming or conventional convex optimization algorithms.

B. Our Approach for CV data Capture and Recovery

In this section, we show our approach for CV data capture and recovery, especially how to select the matrix Ψ to transform the original CV data vector to a sparse one and the matrix Θ that satisfies the RIP of order $2K$ to guarantee an accurate recovery.

Suppose $x \in R^N$ is a vector of CV data samples, e.g., speed samples collected at a fixed rate. According to Equation (1), we need to conduct a transform $\alpha = \Psi^T x$ so that α has a sparse representation in the domain of Ψ . Typical transforms include discrete Fourier transform (DFT), discrete cosine transform (DCT), and Discrete Wavelet Transform (DWT). DCT is a Fourier-based transform similar to DFT, but uses cosine functions and the transformed coefficients are real numbers. DWT is more suitable for piecewise constant signals [16], which is not applicable to fluctuating speed samples. Therefore, we select DCT to transform the CV speed signal [23]:

$$\begin{aligned} \alpha_j &= K(j) \sum_{i=1}^N x_i \cos \frac{\pi j(i-0.5)}{N}, j = 0, \dots, N-1, \\ \text{where } K(j) &= \frac{1}{\sqrt{N}} \text{ when } j = 0, \\ K(j) &= \sqrt{\frac{2}{N}} \text{ when } 1 \leq j \leq N-1. \end{aligned} \quad (7)$$

Next, we need to select a matrix Θ in order to obtain the sampled vector $y \in R^M$ (i.e., Equation (2)). As we mentioned before, Θ should satisfy the RIP of order $2K$ so that the original vector x can be recovered. The previous studies have shown the following theorem:

Theorem 1 [24] Suppose an $M \times N$ matrix Θ is obtained by selecting M rows independently and uniformly at random from the rows of an $N \times N$ unitary matrix U . By normalizing the columns to have unit l_2 norms, Θ satisfies the RIP with probability $1 - N^{-o(\delta_{2K}^2)}$ for every $\delta_{2K} \in (0,1)$ provided that

$$M = \Omega(\mu_U^2 K \log^5 N), \quad (8)$$

where $\mu_U = \sqrt{N} \max_{i,j} |u_{i,j}|$ is called the coherence of the unitary matrix U .

Following Theorem 1, we select an $N \times N$ inverse discrete cosine transform (IDCT) matrix Ψ as the unitary matrix U , and randomly select its M rows to form the matrix Θ . This allows us to skip the DCT and IDCT transforms and be able to acquire M samples (i.e., y) directly from the real observations x as the following:

$$y = \Theta\alpha = D\Psi\Psi^T x = Dx, \quad (9)$$

where $\Theta = D\Psi$ represents a random subset of M rows of an $N \times N$ identity matrix.

Finally, after determining matrix Ψ and Θ , our approach can be summarized as follows. Suppose a CV is capturing speed samples at a fixed rate, we keep a sample if it is generated from a uniform distribution over $[0,1]$ and less than or equal to the compression ratio M/N . When the full data are needed for certain applications, they can be reconstructed by solving the l_1 -norm optimization problem defined in Equation (6). We show the applications of our approach in the following two case studies.

III. CASE STUDY-CAPTURE AND RECOVERY OF 10 MILLION BSM SPEED SAMPLES

The first case study focuses on efficient capture and accurate recovery of 10 million real-world BSM speed samples with the CS approach. The recovery performances regarding other BSM variables are also evaluated in detail.

A. Dataset Introduction

In the SPMD program, BSMs are generated by each CV at 10 Hz according to the SAE J2735 standard [4]. A BSM includes the device ID, timestamp, latitude, longitude, vehicle speed, vehicle heading, yaw rate, and radius of curve. In addition, a BSM includes a "steady state confidence level", which indicates the measurement accuracy, for example, a high confidence level value is commonly found on straight roadways

when the CV is in a steady state [25]. In total, we have extracted 10 million BSM speed samples. The basic statistics of our dataset are listed in Table 1.

TABLE 1
BASIC STATISTICS OF 10 MILLION BSM SPEED SAMPLES

Time Period	04/01/2013 – 04/03/2013
CV Number	~ 3000
Trip Number	16798
Mean (MPH)	38.54
Standard Deviation (MPH)	24.22

In order to protect the privacy of the SPMD participants, Personally Identifiable Information (PII) is removed from our dataset. Our dataset consists of 16798 continuous trips, conforming the 10 Hz sampling rate. The mean and standard deviation of the trip speeds are 38.54 MPH and 24.22 MPH, respectively.

B. Sparsity Analysis

Next, we conduct a sparsity analysis of our dataset. As an illustration, Fig. 1(a) and 1(b) show a set of BSM speed samples x with $N = 1000$ and the corresponding DCT coefficients α . Only 157 out of 1000 coefficients are greater than 1, while the others are negligible. This indicates α is indeed sparse, implying we can apply our approach to capture CV data via a lower sampling rate.

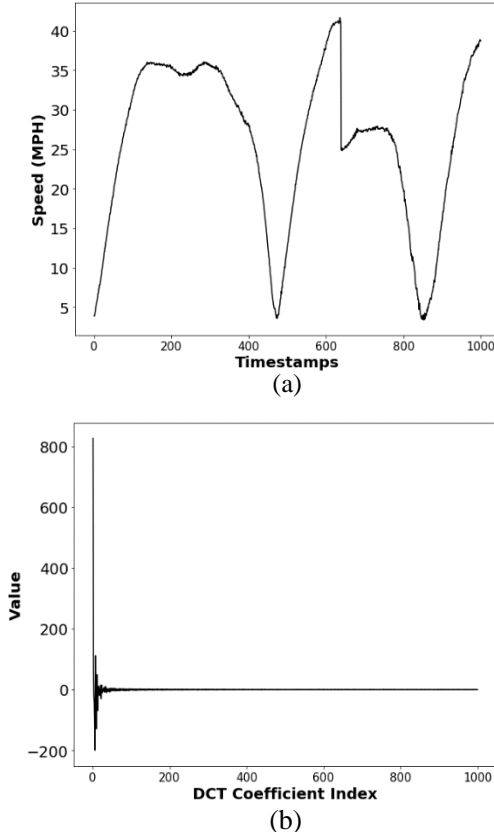


Fig. 1. (a) the original 1000 BSM speed samples; (b) the 1000 DCT coefficients.

C. Recovery Accuracy Evaluation Criterion

When the full data are needed for a certain application such

as travel time estimation, we can recover it by solving Equation (6) to convert $y \in R^M$ to the coefficients in DCT domain $\alpha \in R^N$. The IDCT is then performed on α to obtain the recovered data $\hat{x} \in R^N$. The entire recover process can be easily implemented in parallel. The overall recovery accuracy is measured by calculating the root mean squared error (RMSE) normalized with respect to the l_2 -norm of the entire data series [16]:

$$RMSE = \frac{\|x_o - \hat{x}_r\|_2}{\|x_o\|_2}, \quad (10)$$

where x_o is the original 10 million speed samples and \hat{x}_r is the recovered BSM speed data.

D. Recovery Performance related to M and N

The key parameters of our approach are M and N , which determine the compression ratio and affect the recovery accuracy. Fig. 2(a) shows the RMSEs of the 10 million speed samples under different compression ratios.

When the compression ratio is 0.1, the RMSE of $N = 1000$ is the lowest. Increasing the compression ratio, the RMSEs become lower and close to each other for different values of N . When the compression ratio is greater than 0.2, the RMSEs are capped at 0.025. When the compression ratio reaches 0.6, all the RMSEs are close to zero.

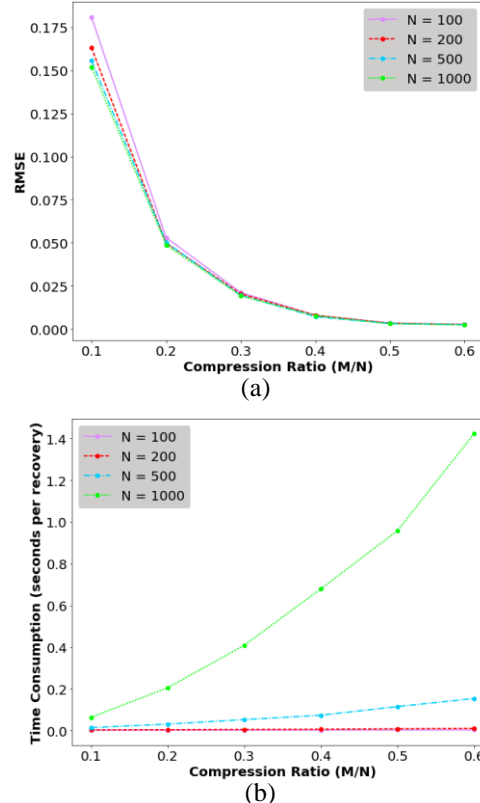


Fig. 2. (a) RMSE by compression ratio (M/N); (b) Time per recovery by compression ratio (M/N).

The computational complexity of l_1 -norm optimization in Equation (6) is $O(N^3 + MN^2)$ [21]. The average time per

recovery is also calculated and shown in Fig. 2(b). All experiments are conducted in Windows 10, using i7-6820HK CPU and 64 GB RAM.

The time per recovery is close to zero for all compression ratios when $N = 100$ and $N = 200$. When $N = 500$ and $N = 1000$, the curves of time per recovery have a large increase under larger compression ratios. In particular, the time is higher than 1.4 seconds per recovery when the compression ratio is equal to 0.6 and $N = 1000$.

As a result of the above analysis of RMSEs and computational efficiency, we select $M = 40$ and $N = 200$ for this case study. The corresponding RMSE calculated using Equation (10) under these parameter values is about 0.05.

To visualize the effect of our approach on CV data collection, a trip made by CV number “2300” is selected. The trip originally has 4967 speed samples. After applying the compression ratio 0.2 ($M=40$ and $N=200$), only 993 samples are retained. Fig. 3(a) shows locations of some original speed samples which are marked in black while Fig. 3(b) shows locations of the samples distilled using our approach which are marked in red. Fig. 3(c) further shows the original 4967 speed samples (black) and the corresponding recovered samples (red). The recovered data highly resemble the original data with only 0.02 RMSE.

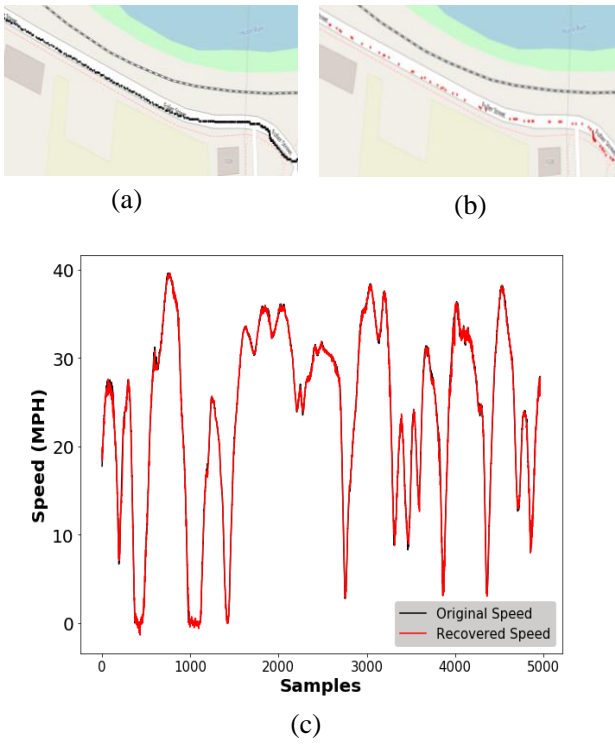


Fig. 3. (a) Locations of original speed samples (black), (b) Locations of compressed speed samples from the CS approach (red), and (c) Original and recovered speed samples.

E. Recovery Performance related to Other BSM Variables

We have further explored the recovery performances of our approach related to other BSM variables, e.g., various speed categories. To be specific, we split the original 10 million speed samples into 8 categories by every 10 MPH and calculate the

corresponding RMSE and the number of samples in each category. As shown in Fig. 4(a), most speed categories have more than 1 million samples except the “11--20” and “51--60” categories. The RMSE curve decreases substantially when the speed category increases. This implies our approach performs better in high speed situations. Note that the actual traffic states of the original data are unknown. So, it may not be reasonable to apply the speed category as the proxy of actual traffic states.

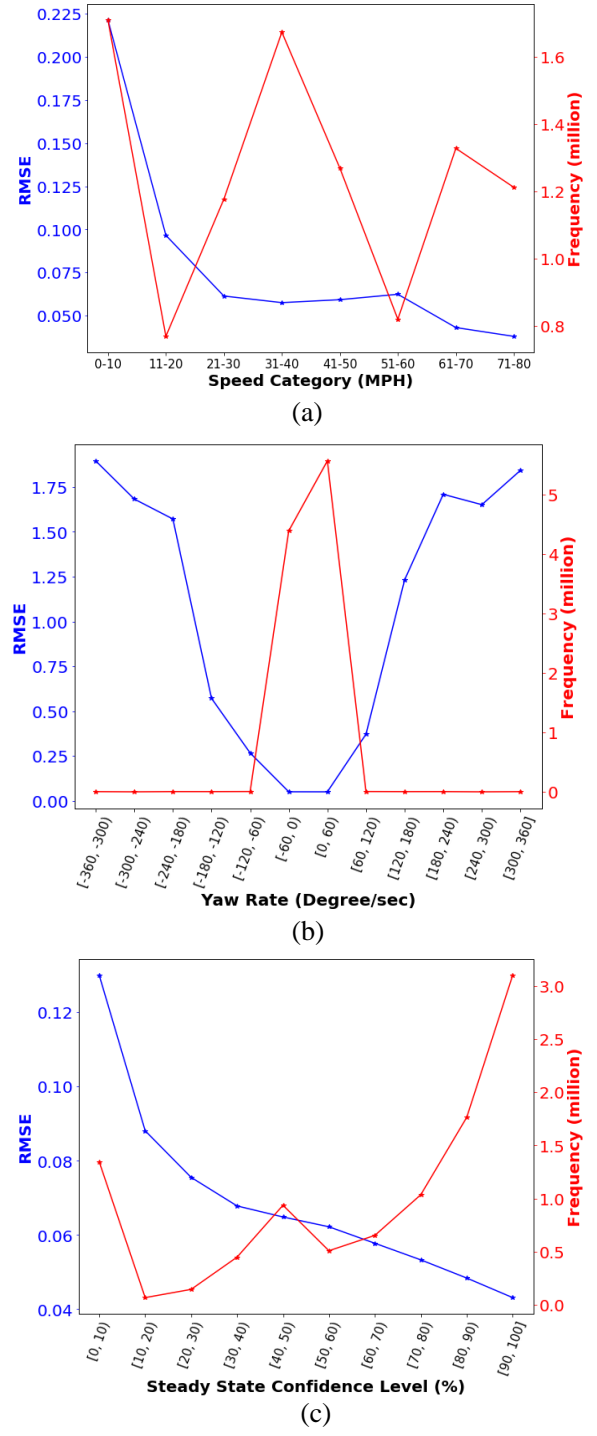


Fig. 4. (a) Recovery performance by speed category, (b) Recovery performance by yaw rate category, and (c) Recovery performance by steady state confidence level category.

Additionally, we evaluate the recovery performance of our approach in terms of driving conditions categorized by yaw rate. In total, there are 12 yaw rate categories from $[-360, 360]$ at 60 degrees interval. Fig. 4(b) shows the RMSEs and the number of samples in each yaw rate category. A negative yaw rate meaning a CV is turning to the left while a positive value indicates turning to the right [25]. A large amount of yaw rates falls into $[-60, 0)$ and $[0, 60)$ categories. For other categories, only few thousands of samples exist. The RMSEs are close to zero for the categories of $[-60, 0)$ and $[0, 60)$ and become larger when the yaw rate is higher.

Last, we examine the correlation between the recovery accuracy using our approach and the BSM variable “steady state confidence level”. We uniformly divide the confidence level interval $[0, 100]$ into 10 categories. Fig. 4(c) shows the RMSEs and number of samples for each steady state confidence level category. There are more samples in higher steady state confidence level categories: about 5 million speed samples have more than 80% confidence level. The RMSE curve decreases when the confidence level increases. This shows the quality of the CV data impacts the recovery performance. Data with higher measurement error cannot be recovered as accurately as those with minor measurement error.

In this case study, we have evaluated our approach using 10 million BSM speed data from the SPMD program. The performances including the RMSE and time per recovery are shown under different settings of the CS parameters M and N . The recovery performances related to other BSM variables are evaluated in detail. However, it is impossible to evaluate the impact of our approach on a certain application without ground truth traffic data such as travel time estimation. Therefore, in the next case study, we build a traffic simulation model for such a purpose.

IV. CASE STUDY-IMPACT OF OUR APPROACH ON TRAVEL TIME ESTIMATION

In this study, we evaluate the impact of our approach on travel time estimation through a traffic simulation model. Travel time estimation aims to provide the travel time from one point to another in a link for a certain time interval [26]. Accurate and reliable travel time estimation plays a critical role in active traffic management [27].

A. Travel Time Estimation from Various Data Sources

Using a simulation model, for each segment s and each time interval j , we can estimate travel times from three data sources: traditional loop detector data, CV data captured at a fixed rate, and CV data via our CS approach. For convenience, these travel times are referred to as $TT_{LP}^{s,j}$, $TT_{CV}^{s,j}$ and $TT_{CS}^{s,j}$ here after. Because the trajectory data of each vehicle are also available, we can obtain the ground truth travel times denoted as $TT_{GR}^{s,j}$ can also be acquired. The computation of these quantities is as follows:

$$TT_d^{s,j} = \frac{L_s}{\bar{v}_d^{s,j}}, \quad (11)$$

where $d = GR, LP, CV$ or CS , indicating the data sources; L_s is the length of segment s ;

$\bar{v}_d^{s,j}$ is the space mean speed over the segments s at time interval j based on data source d .

The space mean speed $\bar{v}_d^{s,j}$ has been calculated in two ways in the literature. Double-loop detector is one of the main sources to measure the vehicle speed [28]. In this case, $\bar{v}_d^{s,j}$ is defined as the harmonic mean of the speeds of vehicles passing the loop detector at the end of segment s during a time interval j , which is calculated as [29].

$$\bar{v}_d^{s,j} = \frac{N_{s,j}}{\sum_{i=1}^{N_{s,j}} \frac{1}{v_{i,j}}}, \quad (12)$$

where $d = LP$;

$N_{s,j}$ is the number of vehicles passing the loop detector at the end of segment s at time interval j ;

$v_{i,j}$ is the speed of vehicle i passing the loop detector at the end of segment s at time interval j .

When the trajectory data from probe vehicles such as CVs are available, some studies define the space mean speed as the average of the mean speeds of all probe vehicles over segment s at an instant of time t within a time interval j [16], [18]:

$$\bar{v}_d^{s,j} = \frac{\sum_{t=1}^{T_j} \left(\frac{\sum_{i=1}^{N_{s,t}} v_{i,s,t}}{N_{s,t}} \right)}{T_j}, \quad (13)$$

where $d = GR, CV$ or CS represents the data source for providing the data;

T_j is the number of total time steps of time interval j ;

$N_{s,t}$ is the number of probe vehicles at segment s at time step t ;

$v_{i,s,t}$ is the speed of probe vehicle i at segment s at time step t .

B. Traffic Simulation Model Setup

To evaluate the impact of our approach on travel time estimation, we have built a simulation model for a five-mile two-lane freeway segment using SUMO. SUMO is an open-source microscopic simulator, which provides rich inter-vehicle interactions [31]. The layout of the freeway segment is shown in Fig. 5.

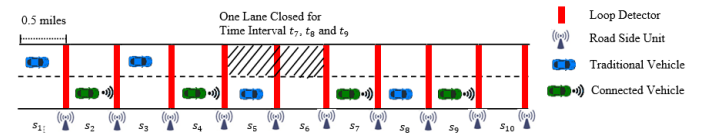


Fig. 5. Five-mile two-lane freeway segment.

The five-mile freeway segment consists of 10 small segments from s_1 to s_{10} at a length of 0.5 miles. One loop detector and one RSU are simulated at every 0.5 mile. The total

simulation time is 3600 seconds, and the traffic demand is set to be 2400 vehicles for the whole simulation process. The traditional vehicles (blue) and CVs (green) are generated based on a predefined CV penetration rate. The simulation period has been split into 12 time intervals at 300 seconds interval, namely, t_1, \dots, t_{12} . The first 3 time intervals are considered as the warming-up stage thus excluded from the analysis. In time intervals t_7, t_8 and t_9 , we close the inner lanes of segment s_5 and s_6 to create congestion conditions. Additional assumptions are listed in the following:

1. CV On-board Units (OBUs) are assumed to have a limited capacity. According to Kianfar and Edara (2013), the OBU can store up to 30 snapshots including the vehicle speed, location, and the time stamp according to the SAE J2735 standard are stored [30]. In this case study, we conduct analysis under different OBU snapshot capacities.

2. If the OBU capacity is reached before the CV passes a road-side unit (RSU), earlier recordings will be replaced by later snapshots, causing information loss [32].

3. When a CV passes a RSU, all recorded snapshots are transmitted to the RSU instantly. A RSU can communicate with multiple CVs at the same time [32]. No transmission loss or delay are considered.

4. All loop detectors and RSUs used in the simulation model operate normally. The loop detectors can record accurate vehicle speeds.

5. After the CV data captured using our approach are transmitted to RSUs and uploaded to the transportation management center, the recovery operation is executed. Travel times are then estimated using the recovered CV data.

C. Travel Time Estimation Accuracy Evaluation Criterion

Using Equations (12) - (14), the overall Mean Absolute Percentage Errors (MAPE) of travel time estimations TT_{LP} , TT_{CV} or TT_{CS} can be calculated as follows:

$$MAPE_d = \frac{\sum_{s=2}^N \sum_{j=4}^T \frac{|TT_d^{s,j} - TT_{GR}^{s,j}|}{TT_{GR}^{s,j}}}{(N-1)*(T-3)}, \quad (14)$$

where $d = LP, CV$ or CS indicates the three data sources for travel time estimations;

$N = 10$ because there are the 10 small segments, each with the length of 0.5 miles;

$T = 12$ because the simulation time is split into 12 time intervals at 300 seconds interval;

i starts from 2 because vehicles enter the segment s_1 with a speed of zero in SUMO;

j starts from 4 because the first 3 time intervals are considered as the warming-up stage.

D. Sensitivity Analysis

There are various parameters that can be adjusted in the simulation model: OBU Capacity, Compression Ratio, CV Data Capture Rate, CV MPR and Arrival Rate.

We first set the CV MPR at a fixed value 0.6 and define an OBU capacity set as $\{50, 100, 150, 200, 250, 300\}$ snapshots, a

CV data capture rate set as $\{1, 10\}$ Hz, a Compression Ratio set as $\{0.2, 0.5\}$ (For the former compression ratio 0.2, M and N are set as 40 and 200; for the latter compression ratio 0.5, M and N are set to 100 and 200, respectively). More specially, two Arrival Rate patterns are tested. One is using a fixed arrival rate 2400 vehicles/hour, and the other is using a varying arrival rate: 1200 vehicles/hour for t_1-t_3 , 2400 vehicles/hour for t_4-t_6 , 4800 vehicles/hour for t_7-t_9 , and 1200 vehicles/hour for $t_{10}-t_{12}$ (the total demand is the same 2400 vehicles for the whole simulation process). Fig. 6 shows the performances of TT_{LP} , TT_{CV} , and TT_{CS} in different scenarios when the CV MPR is 60%. For each scenario, we run the simulation 5 times and compute the average $MAPE_{LP}$, $MAPE_{CV}$ and $MAPE_{CS}$.

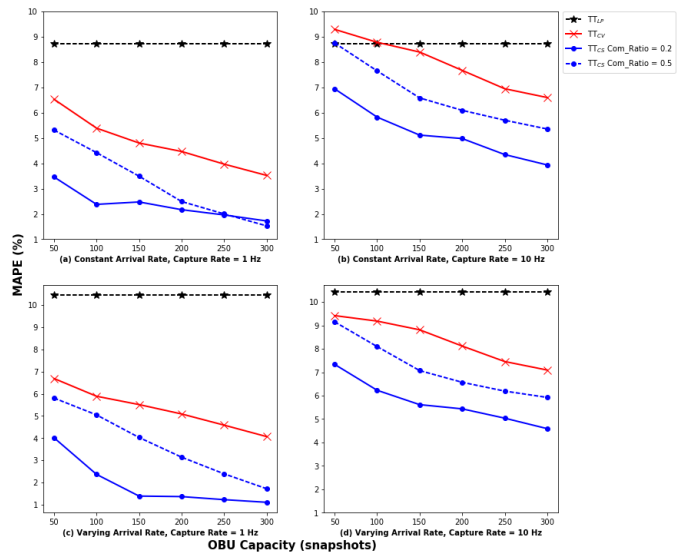


Fig. 6. Travel time estimation performances by OBU Capacity, Arrival Rate, Compression Ratio and Data Capture Rate (CV MPR = 60%).

First, in most scenarios, $MAPE_{CV}$ and $MAPE_{CS}$ are lower than $MAPE_{LP}$, except the few cases when the data capture rate is 10 Hz and the OBU capacity is set to either 50 or 100 snapshots as shown in Fig. 6(b). This is mainly because only limited road information can be stored in a CV at a high data capture rate using a small OBU capacity. One exception is that when CVs collect data via our approach with a compression ratio 0.2, although the OBU capacity is as small as 50, we observe a lower MAPE than TT_{LP} .

Second, as shown in all subplots of Fig. 6, the $MAPE_{CV}$ and $MAPE_{CS}$ curves are decreasing while the OBU capacity is increasing. Using the same simulation setting, $MAPE_{CS}$ is always lower than $MAPE_{CV}$. This is because our approach offers broader spatial-temporal coverage and can accurately recover the CV data. The simulation results verify that trading a little accuracy for broader spatial-temporal coverage is beneficial for travel time estimations using CV data.

Third, comparing Fig. 6(b) to Fig. 6(a), when the data capture rate changes from 10 Hz to 1 Hz, the MAPE performances of TT_{CV} and TT_{CS} are improved. This indicates a higher CV data capture rate (e.g., 10 Hz) may not be necessary for travel time estimation when limited OBU capacity is available. The same observation can be made through the comparison between Fig.

6(d) and Fig. 6(c).

Last, when the data capture rate is 1 Hz, comparing the $MAPE_{CS}$ curves in Fig. 6(a), we observe that for all the OBU capacities except “300”, the one with the compression ratio 0.2 performs better than the one with the compression ratio 0.5. Once again, this is due to the broader spatial-temporal coverage provided by our approach. Similarly, in Fig. 6(c) when the arrival rate varies, the TT_{CS} with a compression ratio 0.2 always performs better than the one with a compression ratio 0.5. This shows a smaller compression ratio does not require the CV to have a large OBU capacity to reach the same travel time estimation accuracy. Therefore, the hardware cost of OBUs can be saved via our technique.

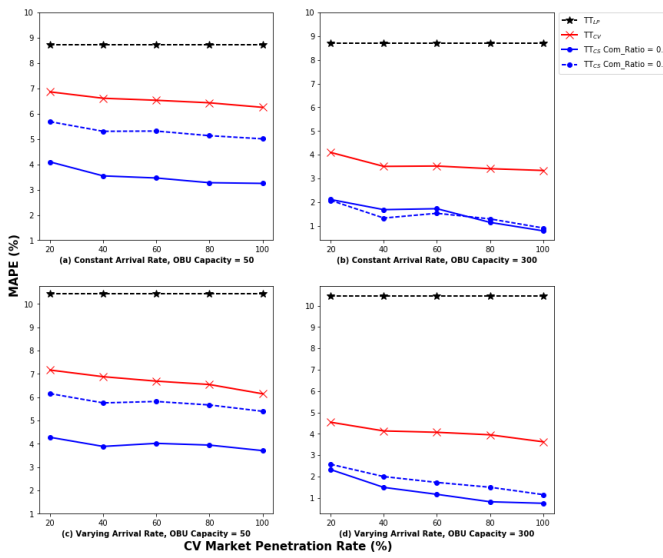


Fig. 7. Travel time estimation performances by OBU Capacity, Arrival Rate, Compression Ratio, CV MPR (CV Data Capture Rate = 1 Hz).

Next, we fix the CV Data Capture Rate at 1 Hz and explore the impact of OBU Capacity, Arrival Rate, Compression Ratio, and CV MPR on travel time estimations. First, the decreasing pattern is not as dramatic as the increasing pattern of CV MPR, no matter the values of other quantities. Second, $MAPE_{CS}$ is consistently lower than $MAPE_{CV}$ in all scenarios, demonstrating the effectiveness of our approach. Third, in Fig. 7(a) and Fig. 7(c) when the OBU Capacity is 50, TT_{CS} with compression ratio 0.2 is more accurate than the value with compression ratio 0.5. In contrast, in Fig. 7(b) and Fig. 7(d) when the OBU capacity is 300, the two $MAPE_{CS}$ curves are closer to each other. This indicates that a lower compression ratio would allow a CV with a small OBU Capacity to cover a larger road segment and a longer period of time. Nevertheless, when the OBU Capacity is big enough, the effect of the compression ratio is not salient.

To further examine our approach’s performance, we fix the CV Data Capture Rate, Compression Ratio, and OBU Capacity and test all combinations of Arrival Rate and CV MPR by running each scenario 5 times. We show the means and standard deviations of $MAPE_{CV}$ and $MAPE_{CS}$ based on the parameter “CV Data Capture Rate-Compression Ratio-OBU Capacity” in Fig. 8(a). The means of $MAPE_{CV}$ and $MAPE_{CS}$ are decreasing,

while the Data Capture Rate is decreasing from 10 Hz to 1 Hz, the Compression Ratio is decreasing from 0.5 to 0.2, and the OBU Capacity is decreasing from 50 to 300 snapshots. The mean of $MAPE_{CS}$ is consistently lower than the mean of $MAPE_{CV}$. Except the scenario of “10-0.5-50”, even the upper bound of $MAPE_{CS}$ is already lower than the lower bound of $MAPE_{CV}$. Fig. 8(b) further calculates the relative reduction by comparing the mean of $MAPE_{CS}$ to the mean of $MAPE_{CV}$. The result shows that when Data Capture Rate is 10 Hz, the heights of the relative reduction bars are always lower than 40%; generally, the relative reduction is higher when the Data Capture Rate is 1 Hz; especially, the relative reduction ranges from 43% to 65% when the “Data Capture Rate-Compression Ratio-OBU Capacity” changes from “1-0.2-50” to “1-0.2-300”.

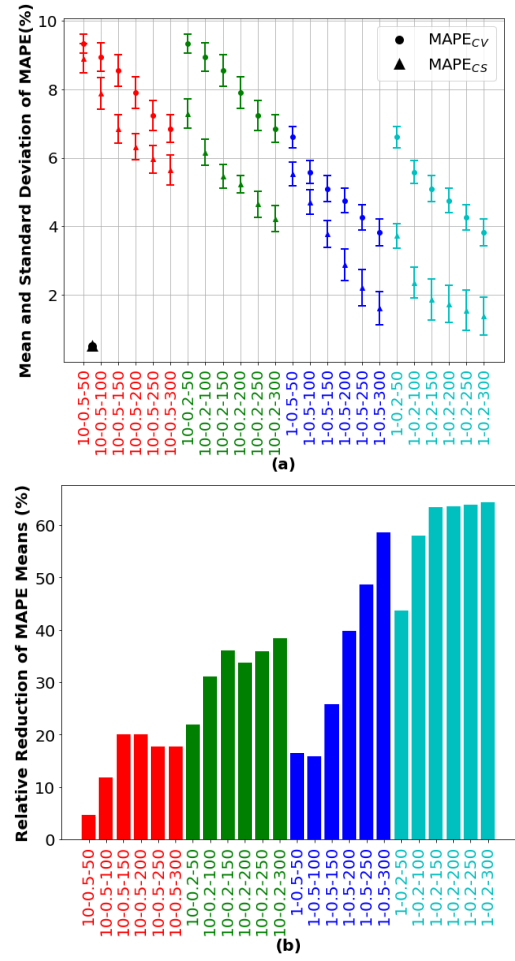


Fig. 8. (a) Mean and standard deviation of $MAPE_{CV}$ and $MAPE_{CS}$ by CV Data Capture Rate-Compression Ratio-OBU Capacity, and (b) Relative reduction of comparing means of $MAPE_{CS}$ and $MAPE_{CV}$ by CV Data Capture Rate-Compression Ratio-OBU Capacity.

E. Impact of Lane Closing

Recall the simulation process, the inner lanes in s_5 and s_6 are closed during the time interval t_7 , t_8 , and t_9 . Fig. 9 shows the color map of the ground truth vehicle speed by segment and time interval from simulation results with constant arrival rates. Starting from the time interval t_7 , a shockwave is observed moving backwards from the upstream segment s_4 to s_2 , where the traffic state changed from a free-flow state to a congestion

state.

In order to evaluate the impact of the traffic state transition on travel time estimations, we compute the $MAPE_{CS}$ and $MAPE_{CV}$ by segments and time intervals when CV MPR = 60% and OBU capacity = 300. The results are shown in Fig. 10. Due to the congestion, travel time estimations are of the least accuracy on the upstream segments s_2 – s_4 since the 8th time interval. In both Fig. 10(a) and Fig. 10(b), the highest MAPE occurs at Segment 3 at the 9th time interval. Comparing Fig. 10(a) to Fig. 10(b), in most cases, travel times TT_{CS} are more accurate than TT_{CV} on the upstream segments starting from the 8th time interval. This is because with limited OBU capacity, if a CV is collecting data at a fixed rate and is stuck in traffic jam, the OBU will be saturated with close to 0 speed readings. Our approach, in comparison, offers a broader spatial-temporal coverage, hence the more accurate result reflected by the lower MAPE.

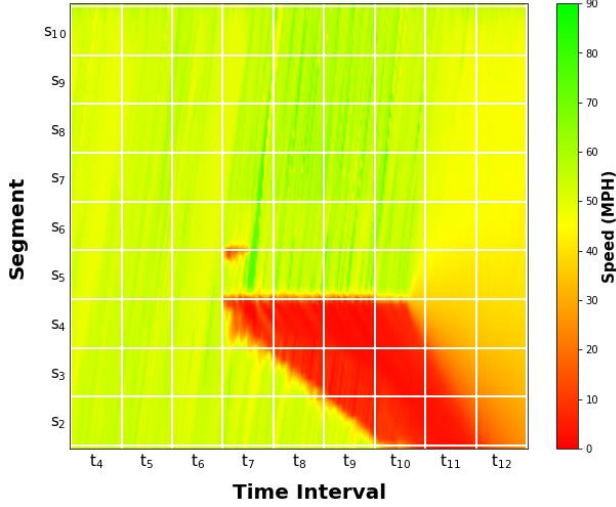


Fig. 9. Colormap of ground truth vehicle speed by segment and time interval.

V. CONCLUSION AND FUTURE RESEARCH DIRECTIONS

As connected vehicles (CVs) emerge, huge amount of data are being collected, stored, and transmitted. Among them, there exists possible redundant information overwhelming storage and communication systems and resulting in prohibitive costs. To mitigate the issue, we propose a Compressive Sensing (CS) based approach for CV data collection and recovery. Our technique allows CVs to compress the data in real-time and can accurately and efficiently recover the original data. We have evaluated our approach using two comprehensive case studies, which demonstrate the effectiveness and efficiency of our approach in addition to applications such as travel time estimation.

In the first case study, 10 million Basic Safety Message speed samples are extracted from the SPMD program. When the compression ratio is 0.2 ($M = 40$ and $N = 200$), our approach can efficiently recover the original speed data with the RMSE as low as 0.05. We have evaluated the recovery performances of our approach related to the speed, yaw rate, and steady state confidence level. The results show our approach works better when the CV is driving with a high speed or a low yaw rate; the approach also performs better with a high steady state

confidence level, which indicates the measurement error is small.

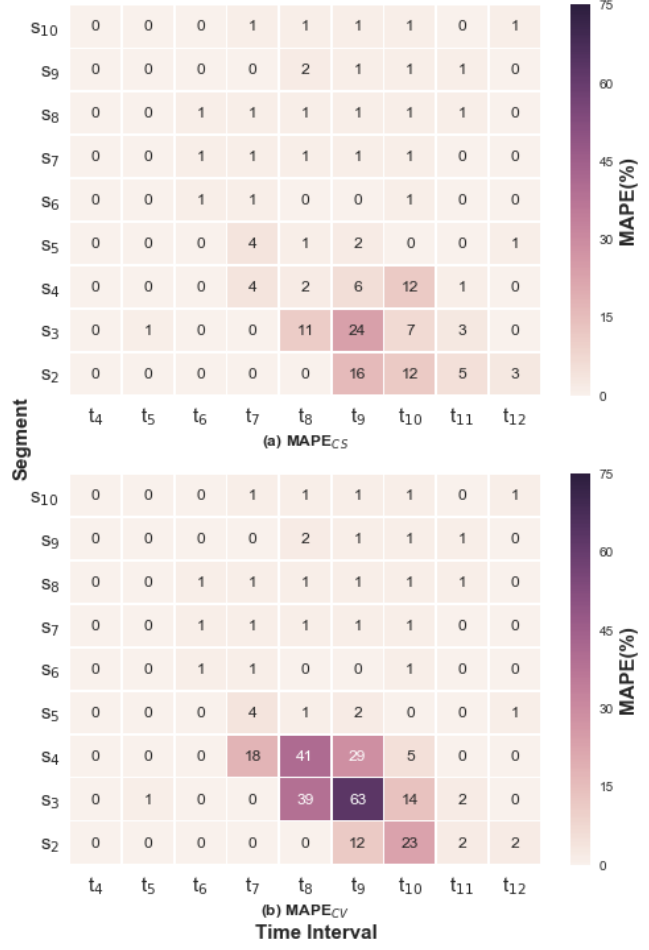


Fig. 10. MAPEs by segment and time interval (CV MPR = 60%, OBU Capacity = 300, Data Capture Rate = 1 Hz).

In the second case study, we build a five-mile two-lane freeway simulation model to evaluate the impact of our approach on travel time estimation. The free-flow and congestion conditions are created by shutting down one lane in the middle of the freeway for certain periods of time. Multiple scenarios under various CV Market Penetration Rates, On-board Unit Capacities, Compression Ratios, Arrival Rates, and Data Capture Rates are simulated. In each scenario, we estimate travel times from different sources: traditional loop detector data, CV data collected with a fixed rate, and CV data using our approach. By comparing to the ground truth values, our approach consistently obtains the lowest MAPE. For certain scenarios, the relative MAPE reduction of applying our approach instead of the conventional data collection method can reach 43% to 65%. The study also shows that our approach offers broader spatial-temporal coverage when used with a small compression ratio. In addition, our technique can recover travel times accurately using a small OBU capacity and scales gracefully when the OBU capacity increases. This implies the OBU cost can be reduced via our technique. Last, our approach significantly improves the estimation accuracy in a congested environment.

There are several future research directions. First, we would like to test the impact of our approach on other CV applications such as information propagation through real-time V2V communications. Next, the CS approach can be applied for multi-modal data capture of autonomous vehicle (AV), which have multiple sensors such as cameras and LIDAR. In addition, the network simulator NS-3 can be incorporated to build more realistic simulation scenarios. Furthermore, we would like to study the impact of factors such as the transmission loss and delay on our approach. Last, it would be interesting to derive a dynamic compression ratio (M/N) based on data qualities and driving conditions such as low steady states and speeds.

REFERENCES

- [1] L. Lin, Q. Wang, and A. W. Sadek, "A novel variable selection method based on frequent pattern tree for real-time traffic accident risk prediction," *Transportation Research Part C: Emerging Technologies*, vol. 55, pp. 444–459, Jun. 2015.
- [2] L. Lin, Q. Wang, and A. W. Sadek, "A combined M5P tree and hazard-based duration model for predicting urban freeway traffic accident durations," *Accident Analysis & Prevention*, vol. 91, pp. 114–126, Jun. 2016.
- [3] L. Lin, Q. Wang, S. Huang, and A. W. Sadek, "On-line prediction of border crossing traffic using an enhanced Spinning Network method," *Transportation Research Part C: Emerging Technologies*, vol. 43, pp. 158–173, Jun. 2014.
- [4] D. Bezzina and J. Sayer, "Safety pilot model deployment: Test conductor team report." [Online]. Available: <https://www.nhtsa.gov/sites/nhtsa.dot.gov/files/812171-safetypilotmodeldeploydeltestcondrtmrep.pdf>. [Accessed: 10-Feb-2018].
- [5] Hitachi, "Connected cars will send 25 gigabytes of data to the cloud every hour," *Quartz*, 2017.
- [6] J. Muckell, P. W. Olsen, J.-H. Hwang, C. T. Lawson, and S. S. Ravi, "Compression of trajectory data: a comprehensive evaluation and new approach," *Geoinformatica*, vol. 18, no. 3, pp. 435–460, Jul. 2014.
- [7] D. H. Douglas and T. K. Peucker, "Algorithms for the Reduction of the Number of Points Required to Represent a Digitized Line or its Caricature," *Cartographica: The International Journal for Geographic Information and Geovisualization*, Oct. 2006.
- [8] K.-F. Richter, F. Schmid, and P. Laube, "Semantic trajectory compression: Representing urban movement in a nutshell," *Journal of Spatial Information Science*, vol. 2012, no. 4, pp. 3–30, Jun. 2012.
- [9] I. S. Popa, K. Zeitouni, V. Oria, and A. Kharrat, "Spatio-temporal compression of trajectories in road networks," *Geoinformatica*, vol. 19, no. 1, pp. 117–145, Jan. 2015.
- [10] K. Wunderlich, "Dynamic Interrogative Data Capture (DIDC) Concept of Operations | National Operations Center of Excellence." [Online]. Available: <https://transportationops.org/publications/dynamic-interrogative-data-capture-didc-concept-operations>. [Accessed: 23-Oct-2017].
- [11] B. Placzek, "Selective data collection in vehicular networks for traffic control applications," *Transportation Research Part C: Emerging Technologies*, vol. 23, no. Supplement C, pp. 14–28, Aug. 2012.
- [12] P. Sebastianov, "Numerical methods for interval and fuzzy number comparison based on the probabilistic approach and Dempster–Shafer theory," *Information Sciences*, vol. 177, no. 21, pp. 4645–4661, Nov. 2007.
- [13] D. L. Donoho, "Compressed sensing," *IEEE Transactions on Information Theory*, vol. 52, no. 4, pp. 1289–1306, Apr. 2006.
- [14] M. M. Abo-Zahhad, A. I. Hussein, and A. M. Mohamed, "Compressive Sensing Algorithms for Signal Processing Applications: A Survey," *International Journal of Communications, Network and System Sciences*, vol. 08, no. 06, p. 197, Jun. 2015.
- [15] E. J. Candes, J. Romberg, and T. Tao, "Robust uncertainty principles: exact signal reconstruction from highly incomplete frequency information," *IEEE Transactions on Information Theory*, vol. 52, no. 2, pp. 489–509, Feb. 2006.
- [16] M. A. Razzaque and S. Dobson, "Energy-Efficient Sensing in Wireless Sensor Networks Using Compressed Sensing," *Sensors*, vol. 14, no. 2, pp. 2822–2859, Feb. 2014.
- [17] K. Li and S. Cong, "State of the art and prospects of structured sensing matrices in compressed sensing," *Front. Comput. Sci.*, vol. 9, no. 5, pp. 665–677, Oct. 2015.
- [18] Z. Li, Y. Zhu, H. Zhu, and M. Li, "Compressive Sensing Approach to Urban Traffic Sensing," in *2011 31st International Conference on Distributed Computing Systems*, 2011, pp. 889–898.
- [19] Z. Zheng and D. Su, "Traffic state estimation through compressed sensing and Markov random field," *Transportation Research Part B: Methodological*, vol. 91, pp. 525–554, Sep. 2016.
- [20] W. Li, D. Nie, D. Wilkie, and M. C. Lin, "Citywide Estimation of Traffic Dynamics via Sparse GPS Traces," *IEEE Intelligent Transportation Systems Magazine*, vol. 9, no. 3, pp. 100–113, Fall 2017.
- [21] R. G. Baraniuk, "Compressive Sensing [Lecture Notes]," *IEEE Signal Processing Magazine*, vol. 24, no. 4, pp. 118–121, Jul. 2007.
- [22] E. J. Candes and M. B. Wakin, "An Introduction To Compressive Sampling," *IEEE Signal Processing Magazine*, vol. 25, no. 2, pp. 21–30, Mar. 2008.
- [23] I. Batal and M. Hauskrecht, "A Supervised Time Series Feature Extraction Technique Using DCT and DWT," in *2009 International Conference on Machine Learning and Applications*, 2009, pp. 735–739.
- [24] W. U. Bajwa, A. M. Sayeed, and R. Nowak, "A restricted isometry property for structurally-subsampled unitary matrices," in *2009 47th Annual Allerton Conference on Communication, Control, and Computing (Allerton)*, 2009, pp. 1005–1012.
- [25] "Safety Pilot Model Deployment Sample Data Handbook.pdf," Dec. 2015.
- [26] U. Mori, A. Mendiburu, M. Álvarez, and J. A. Lozano, "A review of travel time estimation and forecasting for Advanced Traveller Information Systems," *Transportmetrica A: Transport Science*, vol. 11, no. 2, pp. 119–157, Feb. 2015.
- [27] L. Lin, Q. Wang, and A. W. Sadek, "Border crossing delay prediction using transient multi-server queueing models," *Transportation Research Part A: Policy and Practice*, vol. 64, pp. 65–91, Jun. 2014.
- [28] L. Lin, M. Ni, Q. He, J. Gao, and A. W. Sadek, "Modeling the Impacts of Inclement Weather on Freeway Traffic Speed: Exploratory Study with Social Media Data," *Transportation Research Record: Journal of the Transportation Research Board*, vol. 2482, pp. 82–89, Jan. 2015.
- [29] W. Zhang, "Freeway Travel Time Estimation Based on Spot Speed Measurements," Jun. 2006.
- [30] J. Kianfar and P. Edara, "Placement of Roadside Equipment in Connected Vehicle Environment for Travel Time Estimation," *Transportation Research Record: Journal of the Transportation Research Board*, vol. 2381, pp. 20–27, Dec. 2013.
- [31] D. Krajzewicz, J. Erdmann, M. Behrisch, and L. Bieker, "Recent Development and Applications of SUMO - Simulation of Urban MObility," *International Journal On Advances in Systems and Measurements*, vol. 5, no. 3&4, pp. 128–138, Dec. 2012.
- [32] C. Chen, J. Kianfar, and P. Edara, "New Snapshot Generation Protocol for Travel Time Estimation in a Connected Vehicle Environment," *Transportation Research Record: Journal of the Transportation Research Board*, vol. 2424, pp. 1–10, Sep. 2014.



Lei Lin received the B.S. degree in traffic and transportation and the M.S. degree in system engineering from Beijing Jiaotong University, China, in 2008 and 2010, respectively. He received the M.S. degree in computer science and the Ph.D. degree in transportation systems engineering from the University at Buffalo, the State University of New York, Buffalo, in 2013 and 2015, respectively.

From 2013 to 2015, he was a Research Assistant with Transportation Informatics Tier 1 University Transportation Center. He worked as a researcher for Xerox from 2015 to 2017. Since 2017, he has been a research associate at the NEXTRANS Center, Purdue University. His research interests include transportation big data, machine learning applications in transportation, and connected and automated transportation.



Weizi Li received his B.E. degree in Computer Science and Technology from Xiangtan University, China and M.S. degree in Computer Science from George Mason University. He is currently in the doctoral program at the University of North Carolina at Chapel Hill, Department of Computer Science. His research interests include agent-based simulation, intelligent transportation systems, and statistical machine learning.